Available online at www.sciencedirect.com
ScienceDirect
Ceramics International 36 (2010) 1439–1446
CERAMICS INTERNATIONAL
www.elsevier.com/locate/ceramint

Impact of Si and Zr addition on the surface defect and photocatalytic activity of the nanocrystalline TiO_2 synthesized by the solvothermal method

Piyawat Supphasrirongjaroen [a], Piyasan Praserthdam [a], Okorn Mekasuwandumrong [b], Joongjai Panpranot [a,*]

[a] *Center of Excellence on Catalysis and Catalytic Reaction Engineering, Department of Chemical Engineering, Faculty of Engineering, Chulalongkorn University, Bangkok 10330, Thailand*

[b] *Department of Chemical Engineering, Faculty of Engineering and Industrial Technology, Silpakorn University, Nakhonphatom 73000, Thailand*

Received 23 July 2009; received in revised form 30 July 2009; accepted 28 January 2010
Available online 1 March 2010

Abstract

In the present work, the effects of Si and Zr addition on the surface defect and photocatalytic activity of the solvothermal-derived TiO_2 were investigated. The metal-doped TiO_2 samples were prepared with the molar ratio Si/Ti and Zr/Ti ranging from 0.002 to 0.1 and were subjected to two different cooling temperatures (room temperature and 77 K) after calcination as a post-synthesis treatment. The presence of a small amount of metal dopant caused a slight change in the TiO_2 crystallite and BET surface area (ranging from 7.8 to 10.6 nm and corresponding surface area 95 to 159 m^2/g). The photocatalytic activity of TiO_2 did not depend solely on the surface area but rather affected by the concentration of Ti^{3+} on the catalyst surface as shown by a linear ascending trend of the ethylene conversion and the amount of Ti^{3+}/surface area of the catalysts. It is noted that addition of Zr had more positive effect than Si and the effect of post-treatment on the photocatalytic activity of TiO_2 catalysts was more pronounced than the addition of metal dopants.

Keywords: B. Defects; Semiconductor; Nanostructures; Solvothermal; Catalytic properties

1. Introduction

Titanium (IV) dioxide or titania (TiO_2) has a wide range of applications due to its excellent physical and chemical properties. Titania is commercialized as the most powerful photocatalyst because it has high photoactivity for most photocatalytic reactions and is nonexpensive as well as nontoxic to human life [1,2]. The photocatalytic activity of TiO_2 is greatly influenced by its crystal structure, crystallite size, crystallinity, surface area, incident light intensity, and porosity [3]. With the decrease in particle size to nanometer scale, the catalytic activity of titania is enhanced because the optical band gap is widened due to an increase in surface area [4,5], surface defect [6,7], and a shift of the absorption/luminescence spectra towards shorter wavelengths (so-called ''blue shift'').

Surface defects in titania crystal are the results of surface oxygen vacancies, which leave Ti^{3+} sites exposed [8,9]. The surface Ti^{3+} sites play an essential role in photocatalytic process over titania photocatalyst [10–12]. Yamazaki et al. [13] reported that the competitive adsorption of water and ethylene molecules occurred on the same Ti^{4+} sites while the oxygen molecules adsorbed separately on the Ti^{3+} sites. Thus, an increase of Ti^{3+} sites substantially increased oxygen adsorption and photocatalytic oxidation efficiency. In addition, Park et al. [14] showed that the photoelectrons were trapped by the surface defects (Ti^{3+}) leading to the inhibition of the e^-–h^+ recombination. Relationship between the amount of Ti^{3+} defects on TiO_2 surface and their photocatalytic activities have been reported by many authors [15–18].

Many methods have been proposed to synthesize nanocrystalline TiO_2 in anatase phase such as sol–gel [19,20], solvothermal [21] and hydrothermal methods [22]. Solvothermal synthesis, in which chemical reactions occur in aqueous or organic media under the self-produced pressure at low temperature (usually lower than 250 °C), is an advantageous

* Corresponding author. Tel.: +66 2218 6869; fax: +66 2218 6877.
E-mail address: joongjai.p@eng.chula.ac.th (J. Panpranot).

0272-8842/$36.00
doi:10.1016/j.ceramint.2010.02.001

method because it does not require high temperature treatment step that usually causes grain growth, reduction in specific surface area, and phase transformation of the TiO_2 particles as occurred in the sol–gel process [23]. The solvothermal method has been used to successfully synthesize various types of nanosized metal oxides with large surface area, high crystallinity, and high thermal stability [24,25].

Incorporation of metals into anatase phase TiO_2 has been frequently studied as a way to improve the photocatalytic activity of TiO_2 nanoparticles. Addition of a second metal such as silicon [26,27], zirconium [28], tungsten [29], cerium [30] and aluminium [31] has shown to enhance the thermal stability for phase transformation of titania particles from anatase to rutile and increase the surface area of titania. For example [32], anatase-type TiO_2 doped with 4.7 and 12.4 mol% ZrO_2 that were directly precipitated as nanometer-sized particles from acidic precursor solutions of $TiOSO_4$ and $Zr(SO_4)_2$ by simultaneous hydrolysis under hydrothermal conditions at 200 °C, showed higher photocatalytic activity than pure anatase-type TiO_2 for the decomposition of methylene blue. The thermal stability for phase transition from anatase to rutile of TiO_2 doped with ZrO_2 was greatly improved. Cheng et al. [33] reported that silica-doped TiO_2 showed high photocatalytic activity due to the suppression of phase transformation of titania from anatase to rutile and formation of oxygen vacancies.

However, in most of the aforementioned studies, the effect of second metal addition on the photocatalytic activity of TiO_2 was studied at relatively high metal contents (10–50 wt.%). Thus, it is of interest for this study to investigate the effect of second metal addition (Si and Zr) at relatively low metal content (Si/Ti and Zr/Ti molar ratio between 0.002 and 0.1) on both surface defect and photocatalytic activity of the TiO_2-based catalysts. The properties of TiO_2 samples were characterized using various analytical methods such as X-ray diffraction (XRD), N_2 physisorption, electron spin resonance spectroscopy (ESR), and X-ray photoelectron spectroscopy (XPS). Photocatalytic activity of the TiO_2 was tested in a gas-phase decomposition of ethylene under UV irradiation.

2. Experimental

2.1. Preparation of nanocrystalline TiO_2

The TiO_2 catalyst was prepared with a procedure reported by Payakgul et al. [34] using titanium (IV) *n*-butoxide (TNB, Aldrich) as a titanium source. The Si- and Zr-doped TiO_2 were prepared by adding a small amount of TEOS (tetraethylorthosilicate, Aldrich) and zirconium (IV) *n*-butoxide (Aldrich) into the solution of 25 g TNB (Aldrich) in 100 ml toluene, respectively. The molar ratios of Si/Ti and Zr/Ti calculated were in the range 0.002–0.1. Then, set up the test tube in a 300 cm^3 autoclave. The gap between the test tube and the autoclave wall was filled with 30 cm^3 of the same solvent used in the test tube. The autoclave was purged completely by nitrogen before heating up to the desired temperature, in the range of 573 K at a rate of 2.5 K/min. Autogenously pressure during the reaction gradually increased as the temperature was raised. Once the prescribed temperature was reached, the temperature was held constant for 2 h. After the system was cooled down, the resulting powders were repeatedly washed with methanol and dried in air.

2.2. Quenching treatment

The detailed experiment has already been reported in our earlier works [35,36]. Prior to quenching, the synthesized catalysts were calcined in air atmosphere at 573 K with a heating rate of 10 K/min for 1 h, and then it was taken out and immediately quenched in air at room temperature and 77 K. After the samples were quenched, all the catalyst samples were dried in air at room temperature and stored in a desiccator.

2.3. Sample nomenclature

The base samples were TiO_2-RT and TiO_2-77 K which referred to the TiO_2 catalysts without a second metal addition that were cooled down in air at room temperature (RT) and 77 K after calcination, respectively. The nomenclature used for the metal-doped TiO_2, for example "0.002-(Si)-TiO_2-RT" was referred to the Si-doped TiO_2 with Si/Ti molar ratio 0.002 that was cooled down in air at room temperature.

2.4. Characterization

Phase identification and crystallite size of pure and modified nanocrystalline titania were investigated by X-ray diffraction (SIEMENS D5000) using Ni filter Cu K_α radiation from 20° to 80° 2θ. The crystallite size of TiO_2 was determined from half-height width of the 1 0 1 diffraction peak of anatase using the Scherrer equation. The BET surface area was obtained from the N_2 adsorption isotherms measured at 77 K in a Micromeritics ASAP 2000. Electron spin resonance spectroscopy (ESR) was conducted in vacuum at room temperature and without illumination using a JEOL, JES-RE2X electron spin resonance spectrometer. To obtain the "*g*" value, $MnSO_4$ was used as reference standard material. The intensity of ESR was calculated using a computer software program ES-PRIT ESR DATA SYSTEM (version 1.6). The XPS measurement was carried out using an AMICUS photoelectron spectrometer equipped with an Mg K_α X-ray as a primary excitation and KRATOS VISION2 software. XPS elemental spectra were acquired with 0.1 eV energy step at a pass energy of 75 kV. The background pressure during the spectra accumulation was typically 10^{-6} Pa. Detailed spectral scans were taken over Ti 2p, O 1s, Zr 3d, Si 2p and C 1s regions. All the binding energies were referenced to the C 1s peak at 285.0 eV of the surface adventitious carbon.

2.5. Photocatalytic activity measurement

In photocatalytic experiments, the catalysts were packed into a 60 cm long 9 mm diameter horizontal quartz fixed bed reactor. The weights of the catalysts were kept constant at 0.40 g, and in all cases the illuminated length of catalyst was identical. High purity grade air containing 0.1 vol.% ethylene was continuously

fed at a constant flow rate with a gas hourly space velocity (GHSV) of 120 h^{-1}. An air stream with 0.1 vol.% ethylene was first passed through the reactor without irradiation until reaching gas–solid adsorption equilibrium. Then, UV light (λ = 365 nm) was irradiated on the surface of the catalyst using 125 W mercury lamp (Philips, HPLN). The distance between the lamp and the reactor was 20 cm. The light irradiance at surface of the reactor was 0.65 mW/cm^2. The irradiated sample area was approximately 4 cm^2. Analysis of the ethylene feed and other hydrocarbon products were conducted with an on-line SHIMADZU GC-14B gas chromatograph equipped with a flame ionization detector (FID) and VZ-10 column. The retention time of ethylene was approximately around 30 s. Other degradation products such as CO and CO_2 were detected using SHIMADZU GC-8A gas chromatograph equipped with a thermal conductivity detector (TCD) equipped with Molecular sieve 5A and Poropak-Q columns, respectively. Steady state was achieved within ca. 3 h after illumination.

3. Results and discussion

3.1. Textural properties of the TiO_2 photocatalysts

X-ray diffraction patterns of the base TiO_2 and the metal-doped TiO_2 samples with metal/titanium molar ratio 0.1 are shown in Fig. 1. All the samples exhibited the XRD patterns of only pure anatase phase TiO_2 without any contamination of other phases. However, the peak intensities of anatase TiO_2 decreased with the insertion of second metal due probably to the formation of amorphous phases [37]. No diffraction lines of zirconia or silica were observed due to the very small amount and/or the small crystallite sizes of the dopant phase lower than XRD detection limit. Incorporation of Zr and Si into anatase TiO_2 structure has been reported by others [38,39]. The average crystallite sizes of TiO_2 samples were determined from the full

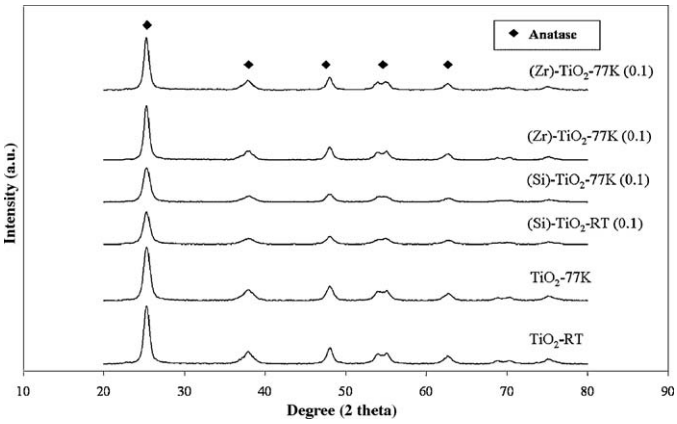

Fig. 1. X-ray diffraction patterns of pure TiO_2 and metal-doped TiO_2.

width at half maximum of the XRD peak at $2\theta = 25^\circ$ using Scherrer's equation. As shown in Table 1, addition of a small amount of Si or Zr to TiO_2 powder, the average crystallite size of TiO_2 decreased slightly from 11.0 to 9.0 nm. It is likely that second metal doping suppressed crystal growth of TiO_2 thus smaller crystallite sizes were obtained. According to the BET analysis, it can be observed that the Si- and Zr-doped TiO_2 samples have larger BET surface area than pure TiO_2. The effect was more pronounced for the Si-doped than the Zr-doped ones. The increase in BET surface area can be related with the lower degree of crystallisation of the mixed oxides with respect to the pure TiO_2. According to Daturi et al. [40], a maximum increase of BET surface area for Zr-modified TiO_2 was observed at the 0.5:0.5 atomic ratio. Thus, we can probably say that addition of relatively small amount of dopant (atomic ratio $\leq$0.1) in this study did not have much impact on the BET surface area of TiO_2 powders. The BET equivalent particle diameters were also calculated and summarized in Table 1. The BET equivalent particle diameters were found to be larger than

Table 1
Physical properties and activities of Si- and Zr-doped TiO_2 samples synthesized by solvothermal method.

Sample nomenclature	BET surface area[a] (m^2/g)	d_{XRD}[b] (nm)	d_{BET}[c] (nm)	Intensity of ESR/BET	Ethylene conversion[d] (%)	TON[e]
TiO_2-RT	93	10.6	16.8	47	21.5	3.6
TiO_2-77 K	97	10.6	16.1	257	34.6	5.6
(Si)-TiO_2-RT (0.002)	159	9.0	9.8	77	23.5	2.3
(Si)-TiO_2-77 K (0.002)	156	9.0	10.0	199	31.5	3.2
(Si)-TiO_2-RT (0.005)	133	8.9	11.7	144	27.9	3.3
(Si)-TiO_2-77 K (0.005)	136	8.6	11.5	213	32.4	3.7
(Si)-TiO_2-RT (0.1)	133	9.0	11.7	56	22.1	2.6
(Si)-TiO_2-77 K (0.1)	136	8.4	11.5	62	22.5	2.6
(Zr)-TiO_2-RT (0.002)	95	9.5	16.4	111	25.7	4.2
(Zr)-TiO_2-77 K (0.002)	99	9.7	15.8	225	33.2	5.2
(Zr)-TiO_2-RT (0.005)	101	7.7	15.5	245	34.5	5.3
(Zr)-TiO_2-77 K (0.005)	106	7.8	14.7	322	39.5	5.8
(Zr)-TiO_2-RT (0.1)	104	8.2	15.0	57	22.2	3.3
(Zr)-TiO_2-77 K (0.1)	105	8.4	14.9	79	23.5	3.5

[a] Determined using BET method.
[b] Determined using Scherrer's equation.
[c] Calculated from $d_{BET} = 6/(SSA \times \rho_p)$, where ρ_p is the weighted density of TiO_2 (3840 kg/m^3).
[d] Photocatalytic reaction was carried out at 313–328 K, 1 bar, and 0.1% ethylene in air.
[e] Turnover number.

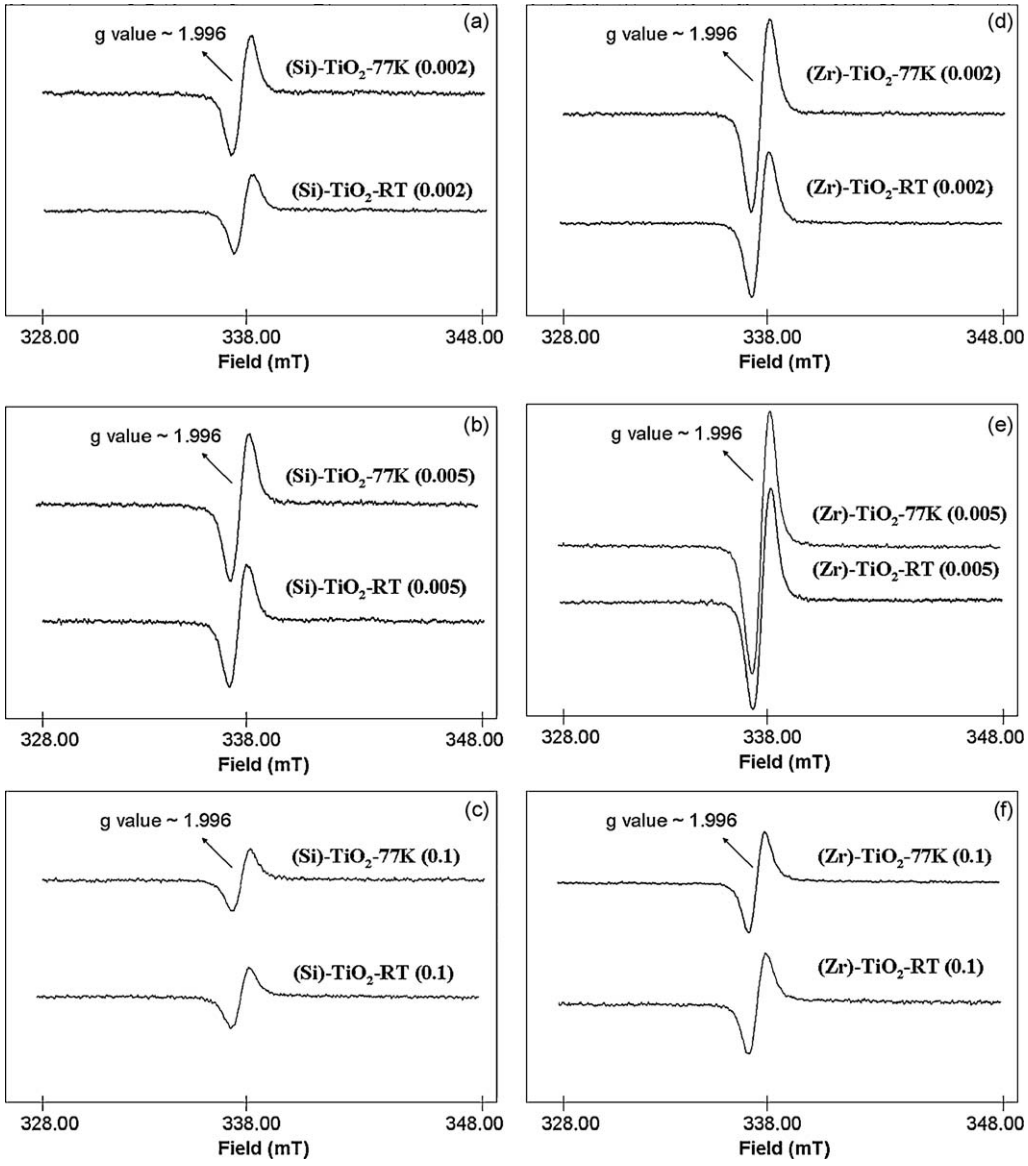

Fig. 2. ESR spectra of (a) 0.002 Si-doped TiO_2, (b) 0.005 Si-doped TiO_2, (c) 0.1 Si-doped TiO_2, (d) 0.002 Zr-doped TiO_2, (e) 0.005 Zr-doped TiO_2, and (f) 0.1 Zr-doped TiO_2.

the ones calculated from XRD results. This can be explained by the agglomeration of TiO_2 particles, which could inhibit the adsorption of N_2 molecules.

It is believed that the process of annealing or calcination has shown to result in a variety of surface defects, strains, and reconstructions of materials [41]. So, the variation of cooling temperature was applied as a post-synthesis treatment with the aim to create more defects on the TiO_2 surface and as a consequence, improve their photocatalytic activities. Moreover, the post-synthesis treatment in cooling temperature did not significantly alter the specific surface area and the average crystallite size of the TiO_2 (see Table 1).

3.2. Electron spin resonance spectroscopy (ESR) study

The number of defective sites of TiO_2 or Ti^{3+} was determined using electron spin resonance spectroscopy technique and the results are shown in Fig. 2. Nakamura et al. [42] and Serwicka [43] reported two signals occurring on the surface of TiO_2 during ESR analysis without illumination indicating: (i) the surface Ti^{3+} and (ii) the bulk defect. Nakaoka and Nosaka [44] reported six signals in ESR measurement on the surface of titania namely (i) $Ti^{4+}OH^-$, (ii) surface Ti^{3+}, (iii) adsorbed oxygen (O^{2-}), (iv) $Ti^{4+}O^{2-}$, (v) inner Ti^{3+}, and (vi) adsorbed water. In the present study, all the TiO_2 samples exhibited similar ESR spectra, in which mainly one signal at the g value of 1.996 was observed. According to Nakaoka et al. [42], this peak was attributed to the Ti^{3+} sites on surface TiO_2. It is clearly seen that the Zr-doped TiO_2 exhibited higher intensity of the ESR signals than the Si-doped ones. The intensity of ESR spectra per surface area of the TiO_2 is given in Table 1. The results indicate that Zr-doped TiO_2 possessed higher concentration of Ti^{3+} defective sites than Si-doped TiO_2.

Table 2
XPS binding energies (eV) and FWHM (eV) values of Si- and Zr-doped TiO_2 catalysts.

Sample nomenclature	Ti 2p		O 1s		Zr 3d		Si 2p	
	BE	FWHM	BE	FWHM	BE	FWHM	BE	FWHM
TiO_2-RT	459.3	1.7	530.8	1.5	–	–	–	–
TiO_2-77 K	459.2	1.7	530.6	1.4	–	–	–	–
(Si)-TiO_2-RT (0.002)	458.8	1.4	530.1	1.5	–	–	102.1	2
(Si)-TiO_2-77 K (0.002)	458.9	1.4	530.2	1.5	–	–	102	1.9
(Si)-TiO_2-RT (0.005)	458.3	1.4	530.1	1.5	–	–	102.1	2.1
(Si)-TiO_2-77 K (0.005)	458.4	1.4	530.2	1.5	–	–	102.1	2.3
(Si)-TiO_2-RT (0.1)	458.5	1.5	530.2	1.6	–	–	102.3	2.2
(Si)-TiO_2-77 K (0.1)	458.6	1.5	530.3	1.6	–	–	102.4	2.1
(Zr)-TiO_2-RT (0.002)	458.5	1.4	530.2	1.5	182.1	1.8	–	–
(Zr)-TiO_2-77 K (0.002)	458.3	1.4	530.1	1.6	182	2	–	–
(Zr)-TiO_2-RT (0.005)	458.3	1.5	530.3	1.4	182.1	1.9	–	–
(Zr)-TiO_2-77 K (0.005)	458.6	1.4	530.3	1.6	182.4	1.8	–	–
(Zr)-TiO_2-RT (0.1)	458.2	1.4	530.1	1.5	182.3	2.2	–	–
(Zr)-TiO_2-77 K (0.1)	458.4	1.4	530.3	1.5	182.1	2.1	–	–

3.3. X-ray photoelectron spectroscopy (XPS) study

It is well known that XPS is a surface probe detecting electrons that are generated from a depth of a few nanometers on the surface of the sample. To make the XPS results comparable to those of ESR measurement, elemental composition and chemical states on the surface of metal-doped TiO_2 samples that were subjected to two different cooling temperatures were studied. The binding energy values and the full width at half maximum (FWHM) values of Zr 3d, O 1s, Si 2p and Ti 2p photoelectron peaks as determined by XPS of the various TiO_2 samples are summarized in Table 2. The binding energies for Si 2p and Zr 3d levels are in agreement with those reported for pure SiO_2 [45] and ZrO_2 [46] at 103.0 and 183.5 eV, respectively. No significant variation has been observed for these elements over the metal-doped TiO_2 samples. However, the binding energy of the Ti 2p band for the metal-doped samples was found to be lower than that of the pure TiO_2. For better comparison, the XPS bands of Ti 2p for Si- and Zr-doped TiO_2 are shown in Fig. 3. Normally, the Ti 2p XPS spectra of TiO_2 sample show two shoulder peaks at lower binding energy (Ti $2p_{3/2}$) and higher binding energy (Ti $2p_{1/2}$), respectively, in line with the earlier reports by Mukhopadhyay and Garofalini [47]. The presence of defect is visible as a shoulder in the XPS spectra which was assigned to Ti^{3+} oxidation state. From Fig. 3, the binding energy of Ti 2p electrons was found to be lower than the value normally published for Ti^{4+} ions in TiO_2 (459.2 eV) [48,49]. However, the Ti 2p spectrum was slightly broadened and a shoulder band appeared at 1.6 eV lower than the Ti^{4+} binding energy, this could be associated with the Ti^{3+} defect state [50].

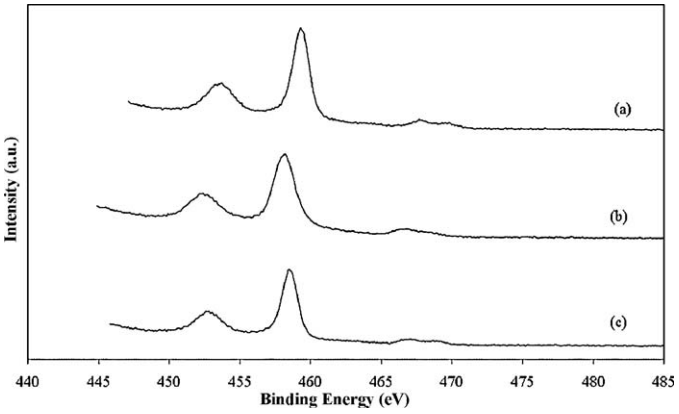

Fig. 3. Ti 2p XPS spectra of various TiO_2 samples: (a) TiO_2-RT, (b) 0.1-(Zr)-TiO_2-RT, and (c) 0.1-(Si)-TiO_2-RT.

3.4. Photocatalytic activity test

The photocatalytic activity of the TiO_2 and metal-doped TiO_2 samples was tested for the photocatalytic decomposition of ethylene in gas-phase under UV illumination. Under these conditions, the only products detected by gas chromatography were CO_2 and H_2O. The mechanism of photocatalytic decomposition of ethylene has been reported by many researchers [13,51]. The mechanism is believed to involve absorption of an UV photo by TiO_2 to produce an electron–hole pair. Both hole and electron play an important role on creating the reaction intermediate, which react further and form CO_2 as the final product.

Photocatalytic activities of the TiO_2 samples with different proportions of Si/Ti and Zr/Ti were evaluated in the decomposition of ethylene in gas-phase and the results are shown in Table 1. In our previous studies [35,36], the effects of cooling media and temperature on the photocatalytic activities of solvothermal-derived TiO_2 have been reported. It was found in this study that the photocatalytic activity of the metal-doped TiO_2 cooled down in different cooling temperatures is also evidently different. The ethylene conversion results show that the metal-doped TiO_2 at lower amounts of metal exhibited higher photocatalytic activity than the pure titania. Ethylene conversions at steady state for the metal-doped TiO_2 samples after cooling at room temperature were ranging from ca. 22% to 39% while pure TiO_2 sample under similar reaction conditions gave ca. 21% ethylene conversion. The turnover number (TON) was calculated from the ratio of the number of photoinduced transformation for a given period of time and the number of

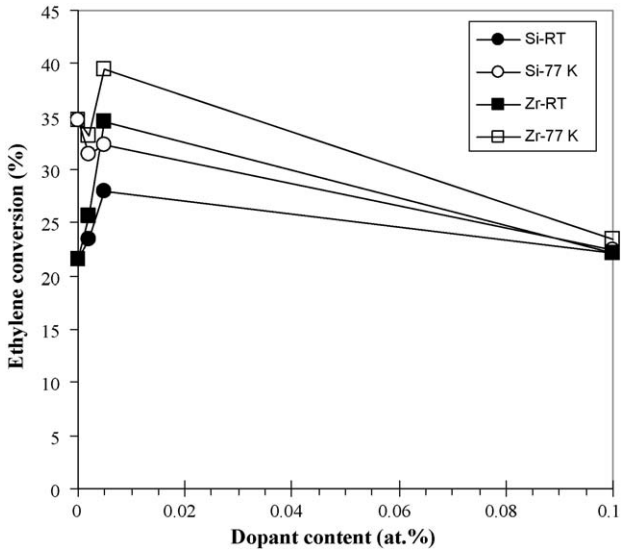

Fig. 4. Plot between ethylene conversion at steady state (ca. 3 h) and dopant content.

photocatalytic sites (surface area). From Table 1, TONs for all the catalysts were greater than unity, the (photo) catalytic character of the reaction or process was confirmed.

The photocatalytic activity of metal-doped TiO_2 depended on the cooling temperature applied after calcination. It was found that metal-doped TiO_2 samples cooled at lower temperature exhibited higher photocatalytic activity than those cooled in high temperature ones. For example, the ethylene conversion of 0.005 Zr-doped TiO_2 was 34.5% and 39.5% for the sample cooled down at room temperature and at 77 K, respectively. Additionally, the metal content has an obvious effect on the activity of the metal-modified TiO_2 catalysts. The plots of ethylene conversion versus metal content (Fig. 4) show that there existed an optimal metal content (atomic ratio) to achieve the highest photocatalytic activity. If the concentration of metal is too low, the promotional effect is not significant while for high metal content, the active sites of TiO_2 may be blocked and lower catalytic activity would be obtained. An optimum metal content on photocatalytic activity of the Zr- and Si-doped TiO_2 has also been suggested by Fu et al. [28] for much higher metal loading range. The specific activity of TiO_2 synthesized by sol–gel method was enhanced by the addition of SiO_2 (optimum at 16 wt.%) or ZrO_2 (optimum at 12 wt.%). The increase in activity of the modified catalysts was attributed to both an increase in surface area (ranging between 250 and 400 m^2/g) and chemical change on the catalyst surface.

The results in this study show that for a similar metal content, the Zr-doped TiO_2 exhibited higher photocatalytic activity than the Si-doped ones. However, one may notice that the Si-doped TiO_2 had larger BET surface areas than the Zr-doped ones and in general, anatase TiO_2 nanoparticles with higher specific surface area typically exhibit higher photocatalytic activity. The increase of surface area means the increase of the number of active sites on which the electron acceptor and donor are adsorbed and participate in the photocatalytic reaction. In our present study, the presence of

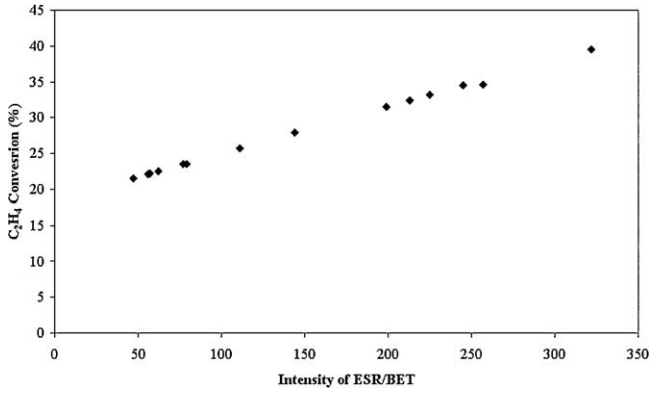

Fig. 5. Photocatalytic activity at steady state (ca. 3 h) of metal-doped TiO_2 for ethylene decomposition as a function of the intensity of ESR/BET.

very small amount of metal dopants caused only a slight change in the TiO_2 crystallite and BET surface area (ranging from 7.8 to 10.6 nm and corresponding surface area 95 to 159 m^2/g). The photocatalytic activity of TiO_2 did not depend solely on the surface area but were found to be correlated well with the concentration of Ti^{3+} on the catalyst surface as illustrated by a linear ascending trend of the ethylene conversion and the amount of Ti^{3+}/surface area of the catalysts in Fig. 5. It should also be noted that the effect of post-treatment on enhancing the concentration of Ti^{3+} on the TiO_2 was more pronounced than the addition of metal dopants.

4. Conclusions

The Si- and Zr-doped TiO_2 with Si/Ti and Zr/Ti molar ratios ranging from 0.002% to 0.1% were prepared via the solvothermal method using titanium *n*-butoxide as the titanium precursor and toluene as the solvent. It was found that selection of a suitable second metal doping can enhance photocatalytic activity of the TiO_2. Based on ESR and XPS analyses, the improved photocatalytic activity of the TiO_2 is suggested to be due to the presence of Ti^{3+} defect sites on the surface of TiO_2. Moreover, a post-synthesis treatment by cooling in air at 77 K effectively enhanced the amount of Ti^{3+} and photocatalytic activity of the TiO_2 and the metal-doped TiO_2.

Acknowledgements

The financial supports from the Thailand Research Fund (TRF) and Commission on Higher Education are gratefully acknowledged.

References

[1] C.H. Chen, E.M. Kelder, J. Schoonman, Electrostatic sol-spray deposition (ESSD) and characterization of nanostructured TiO_2 thin films, Thin Solid Films 342 (1999) 35–41.
[2] A. Fujwashima, T.N. Rao, D.A. Tryk, Titanium dioxide photocatalysis, J. Photochem. Photobiol. C: Photochem. Rev. (2000) 1–21.
[3] B. Ohtani, Y. Ogawa, S. Nishimoto, Photocatalytic activity of amorphous-anatase mixture of titanium(IV) oxide particles suspended in aqueous solutions, J. Phys. Chem. B 101 (1997) 3746–3752.

[4] K.M. Reddy, C.V.G. Reddy, S.V. Manorama, Preparation, characterization, and spectral studies on nanocrystalline anatase TiO_2, J. Solid State Chem. 158 (2001) 180–186.
[5] T. Toyoda, H. Kawano, Q. Shen, A. Kotera, M. Ohmori, Characterization of electronic states of TiO_2 powders by photoacoustic spectroscopy, Jpn. J. Appl. Phys. Part 1 39 (2000) 3160–3163.
[6] C. Shifu, C. Gengyu, The effect of different preparation conditions on the photocatalytic activity of $TiO_2{\cdot}SiO_2$/beads, Surf. Coat. Technol. 200 (2006) 3637–3643.
[7] K. Suriye, P. Praserthdam, B. Jongsomjit, Impact of Ti^{3+} present in titania on characteristics and catalytic properties of the Co/TiO_2 catalyst, Ind. Eng. Chem. Res. 44 (2005) 6599–6604.
[8] G. Lu, A. Linsebigler, J.T. Yates Jr., Ti^{3+} defect sites on TiO_2(1 1 0): production and chemical detection of active sites, J. Phys. Chem. 98 (1994) 11733–11738.
[9] V. Henrich, R.L. Kurtz, Surface electronic structure of TiO_2: atomic geometry, ligand coordination, and the effect of adsorbed hydrogen, Phys. Rev. B 23 (1981) 6280–6287.
[10] U. Diebold, J. Lehman, T. Mahmoud, M. Kuhn, G. Leonardelli, W. Hebenstreit, M. Schmid, P. Varga, Intrinsic defects on a TiO_2(1 1 0)(1 × 1) surface and their reaction with oxygen: a scanning tunneling microscopy study, Surf. Sci. 411 (1998) 137–153.
[11] R. Schaub, P. Thostrup, N. Lopez, E. Laegsgaard, I. Stensgaard, J.K. Norskov, F. Besenbacher, Oxygen vacancies as active sites for water dissociation on rutile TiO_2(1 1 0), Phys. Rev. Lett. 87 (2001) 2661041–2661044.
[12] R. Schaub, E. Wahlstrom, A. Ronnau, E. Laegsgaard, I. Stensgaard, F. Besenbacher, Oxygen-mediated diffusion of oxygen vacancies on the TiO_2(1 1 0) surface, Science 299 (2003) 377–379.
[13] S. Yamazaki, S. Tanaka, H. Tsukamoto, Kinetic studies of oxidation of ethylene over a TiO_2 photocatalyst, J. Photochem. Photobiol. A 121 (1999) 55–61.
[14] D.-R. Park, J. Zhang, K. Ikenue, H. Yanashita, M. Anpo, Photocatalytic oxidation of ethylene to CO_2 and H_2O on ultrafine powdered TiO_2 photocatalysts in the presence of O_2 and H_2O, J. Catal. 185 (1999) 114–119.
[15] F.B. Li, X.Z. Li, Photocatalytic properties of gold/gold ion-modified titanium dioxide for wastewater treatment, Appl. Catal. A 228 (2002) 15–27.
[16] F.B. Li, X.Z. Li, C.H. Ao, S.C. Lee, M.F. Hou, Enhanced photocatalytic degradation of VOCs using Ln^{3+}-TiO_2 catalysts for indoor air purification, Chemosphere 59 (2005) 787–800.
[17] W. Kongsuebchart, P. Praserthdam, J. Panpranot, A. Sirisuk, P. Supphasrirongjaroen, C. Satayaprasert, Effect of crystallite size on the surface defect of nano-TiO_2 prepared via solvothermal synthesis, J. Cryst. Growth 297 (2006) 234–238.
[18] K. Suriye, P. Praserthdam, B. Jongsomjit, Control of Ti^{3+} surface defect on TiO_2 nanocrystal using various calcination atmospheres as the first step for surface defect creation and its application in photocatalysis, Appl. Surf. Sci. 253 (2007) 3849–3855.
[19] K.H. Yoon, J.S. Noh, C.H. Kwon, M. Muhammed, Photocatalytic behavior of TiO_2 thin films prepared by sol–gel process, Mater. Chem. Phys. 95 (2006) 79–83.
[20] C.H. Kwon, H. Shin, J.H. Kim, W.S. Choi, K.H. Yoon, Degradation of methylene blue via photocatalysis of titanium dioxide, Mater. Chem. Phys. 86 (2004) 78–82.
[21] C.-S. Kim, B.K. Moon, J.-H. Park, S.T. Chung, S.-M. Son, Synthesis of nanocrystalline TiO_2 in toluene by a solvothermal route, J. Cryst. Growth 254 (2003) 405–410.
[22] Y.V. Kolen'ko, A.A. Burukhin, B.R. Churagulov, N.N. Oleynikov, Synthesis of nanocrystalline TiO_2 powders from aqueous $TiOSO_4$ solutions under hydrothermal conditions, Mater. Lett. 57 (2003) 1124–1129.
[23] O. Carp, C.L. Huisman, A. Reller, Photoinduced reactivity of titanium dioxide, Prog. Solid State Chem. 32 (2004) 33–177.
[24] S. Kongwudthiti, P. Praserthdam, P.L. Silveston, M. Inoue, Influence of synthesis conditions on the preparation of zirconia powder by the glycothermal method, Ceram. Int. 29 (2003) 807–814.
[25] O. Mekasuwandumrong, P.L. Silveston, P. Praserthdam, M. Inoue, V. Pavarajarn, W. Tanakulrungsank, Synthesis of thermally stable micro spherical χ-alumina by thermal decomposition of aluminum isopropoxide in mineral oil, Inorg. Chem. Commun. 6 (2003) 930–934.
[26] K.Y. Jung, S.B. Park, Enhanced photoactivity of silica-embedded titania particles prepared by sol–gel process for the decomposition of trichloroethylene, Appl. Catal. B: Environ. 25 (2000) 249–256.
[27] S.R. Kumar, C. Suresh, K.A. Vasudevan, N.R. Suja, P. Mukundan, K.G.K. Warrier, Phase transformation in sol–gel titania containing silica, Mater. Lett. 38 (1999) 161–166.
[28] X. Fu, L.A. Clark, Q. Yang, M.A. Anderson, Enhanced photocatalytic performance of titania-based binary metal oxides: TiO_2/SiO_2 and TiO_2/ZrO_2, Environ. Sci. Technol. 30 (1996) 647–653.
[29] H. Yang, D. Zhang, L. Wang, Synthesis and characterization of tungsten oxide-doped titania nanocrystallites, Mater. Lett. 57 (2002) 674–678.
[30] T. López, F. Rojas, R.A. -Katz, F.F. Galindo, A. Balankin, A. Buljan, Porosity, structural and fractal study of sol–gel TiO_2–CeO_2 mixed oxides, J. Solid State Chem. 177 (2004) 1873–1885.
[31] S. Sivakumar, C.P. Sibu, P. Mukundan, P.K. Pillai, K.G.K. Warrier, Nanoporous titania-alumina mixed oxides—an alkoxide free sol–gel synthesis, Mater. Lett. 58 (2004) 2664–2669.
[32] M. Hirano, Ch. Nakahara, K. Ota, O. Tanaike, M. Inagaki, Photoactivity and phase stability of ZrO_2-doped anatase-type TiO_2 directly formed as nanometer-sized particles by hydrolysis under hydrothermal conditions, J. Solid State Chem. 170 (2003) 39–47.
[33] P. Cheng, M. Zheng, Y. Jin, Q. Huang, M. Gu, Preparation and characterization of silica-doped titania photocatalyst through sol–gel method, Mater. Lett. 57 (2003) 2989–2994.
[34] W. Payakgul, O. Mekasuwandumrong, V. Pavarajarn, P. Praserthdam, Effects of reaction medium on the synthesis of TiO_2 nanocrystals by thermal decomposition of titanium (IV) *n*-butoxide, Ceram. Int. 31 (2005) 391–397.
[35] P. Supphasrirongjaroen, P. Praserthdam, J. Panpranot, D. Na-Ranong, O. Mekasuwandumrong, Effect of quenching medium on photocatalytic activity of nano-TiO_2 prepared by solvothermal method, Chem. Eng. J. 138 (2008) 622–627.
[36] P. Supphasrirongjaroen, W. Kongsuebchart, J. Panpranot, O. Mekasuwandumrong, C. Satayaprasert, P. Praserthdam, Dependence of quenching process on the photocatalytic activity of solvothermal-derived TiO_2 with various crystallite sizes, Indust. Eng. Chem. Res. 47 (2008) 693–697.
[37] M. Yoshinaka, K. Hirota, O. Yamaguchi, Formation and sintering of TiO_2 (anatase) solid solution in the system TiO_2–SiO_2, J. Am. Ceram. Soc. 80 (1997) 2749–2753.
[38] M. Inoue, K. Sato, T. Nakamura, T. Inui, Glycothermal synthesis of zirconia–rare earth oxide solid solutions, Catal. Lett. 65 (2000) 79–83.
[39] S. Iwamoto, W. Tanakulrungsank, M. Inoue, K. Kagawa, P. Praserthdam, Synthesis of large-surface area silica-modified titania ultrafine particles by the glycothermal method, J. Mater. Sci. Lett. 19 (2000) 1439–1443.
[40] M. Daturi, A. Cremona, F. Milella, G. Buca, E.J. Vogna, Characterisation of zirconia–titania powders prepared by coprecipitation, Eur. Ceram. Soc. 18 (1998) 1079–1087.
[41] M.A. Henderson, An HREELS and TPD study of water on TiO_2(1 1 0): the extent of molecular versus dissociative adsorption, Surf. Sci. 355 (1996) 151–166.
[42] I. Nakamura, N. Negishi, S. Kutsuna, T. Ihara, S. Sugihara, K. Takeuchi, Role of oxygen vacancy in the plasma-treated TiO_2 photocatalyst with visible light activity for NO removal, J. Mol. Catal. A 161 (2000) 205–212.
[43] E. Serwicka, ESR study on the interaction of water vapour with polycrystalline TiO_2 under illumination, Colloids Surf. 13 (1985) 287–293.
[44] Y. Nakaoka, Y. Nosaka, ESR Investigation into the effects of heat treatment and crystal structure on radicals produced over irradiated TiO_2 powder, J. Photochem. Photobiol. A 110 (1997) 299–305.
[45] H.J.M. Bosman, A.P. Pijpers, A.W.M.A. Jaspers, An X-ray photoelectron spectroscopy study of the acidity of SiO_2–ZrO_2 mixed oxides, J. Catal. 161 (1996) 551–559.
[46] Z. Bastl, A.I. Senkevich, I. Spirovova, V. Vrtilkova, Angle-resolved core-level spectroscopy of Zr1Nb alloy oxidation by oxygen, water and hydrogen peroxide, Surf. Interface Anal. 34 (2002) 477–480.

[47] S. Mukhopadhyay, S. Garofalini, Surface studies of $TiO_2{\cdot}SiO_2$ glasses by X-ray photoelectron spectroscopy, J. Non-Cryst. Solids 126 (1990) 202–208.
[48] P.M. Kumar, S. Badrinarayanan, M. Sastry, Nanocrystalline TiO_2 studied by optical, FTIR and X-ray photoelectron spectroscopy: correlation to presence of surface states, Thin Solid Films 358 (2000) 122–130.
[49] Z. Wei, Q. Xin, X. Guo, E.L. Sham, P. Grange, B. Delmon, Titania-modified hydrodesulphurization catalysts. I. Effect of preparation techniques on morphology and properties of TiO_2–Al_2O_3 carrier, Appl. Catal. 63 (1990) 305–317.
[50] L.Q. Wang, D.R. Baer, M.H. Engelhard, A.N. Schultz, Adsorption of liquid and vapor water on TiO_2(1 1 0) surfaces: the role of defects, Surf. Sci. 344 (1995) 237–250.
[51] A. Sirisuk, C.G. Hill, M.A. Anderson, Photocatalytic degradation of ethylene over thin films of titania supported on glass rings, Catal. Today 54 (1999) 159–164.